MEMOVOLC Scientific Report

Anson Hancock, PhD Student, Lancaster University

Host: Dr. Gaetana Ganci, INGV-Catania

Purpose of Visit

The interpretation of ground-based thermal data is an important tool in the study and monitoring of volcanoes. Unlike satellite-based sensors, ground-based thermal cameras can be placed as situations demands, to cover specific areas for extended periods of time, allowing continuous monitoring of volcanic activity.

While ground-based sensors have many advantages, there are several factors that complicate the analysis of the data they produce. Factors as the surface roughness of the target area and the target path-length (Ball and Pinkerton, 2006) can increase error during the conversion of radiance data to surface temperature. As for space-based sensors, data collected by ground-based cameras must be corrected for atmospheric effects. FLIR systems include a software package with their cameras called FLIR ThermaCam Researcher. Researcher allows the user to input the temperature and relative humidity at the camera as well as the target path-length. The software then uses the LOWTRAN atmospheric correction model to compute emissivity and atmospheric corrections.

The Istituto Nazionale di Geofisica e Vulcanologia (INGV) at Catania, Sicily currently uses a fixed FLIR A320 thermal camera (EMCT) to monitor thermal activity at Mount Etna. The camera is located at Mt Cagliato, approximately 8.5 km away from the summit, and at an elevation of 1.158 km. Ganci et al. (2013) used data collected by the EMCT to calculate radiant heat flux and erupted volume for the Aug 12, 2011 paroxysmal eruption of Etna. To do this, Ganci et al. tried to use the ThermaCam Researcher software to process target pixels within the images, but found that the ThermalCam Researcher limited atmospheric correction processing to a maximum path length of 3.6 km. Thus Ganci et al. used an additional Visual Basic code and the MatLab Polyfit function to represent atmospheric attenuation with distance. They then extrapolated the curve to the actual recorded distance (Fig. 1).

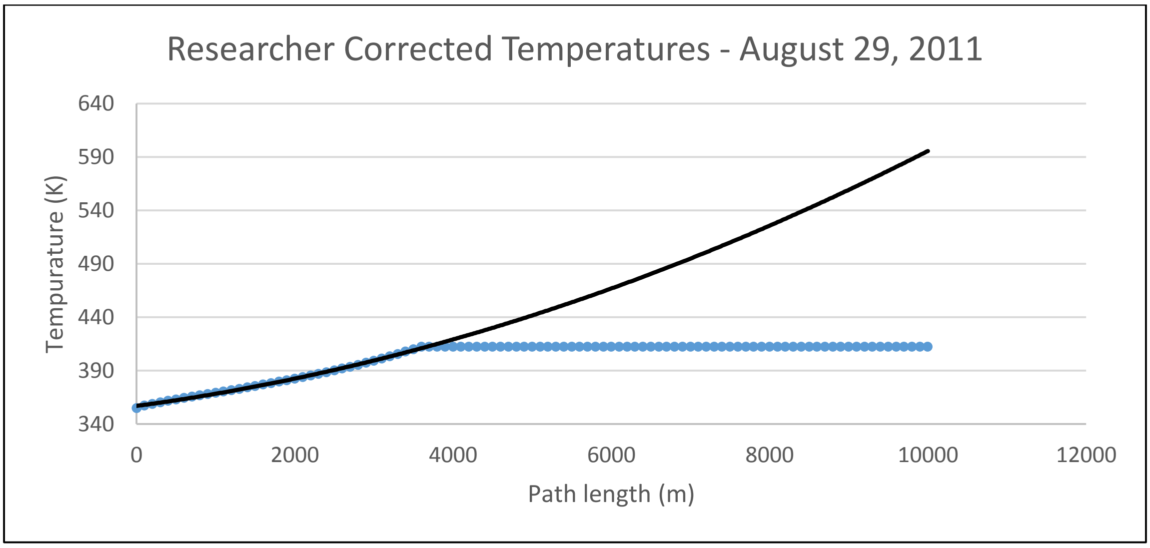

Figure 1 – Regression curve used by Ganci et al. (2013) to extrapolate temperatures beyond the path length correction limit of ThermaCam Researcher: Dotted blue line = EMCT temperatures corrected by Researcher, Black line = 2nd order polynomial regression curve used by Ganci et al.

Several problems can be found in the process used by Ganci et al. (2013). One issue stems from the fact that a constant ambient temperature and relative humidity were assumed along the path length when calculating atmospheric corrections. With increasing target distance, ambient temperature and relative humidity variations are more likely to be significant. If this is the case, then using constant atmospheric conditions when processing data collected from the EMCT camera, which is located approximately 8.5 km away from the target area, would produce error in atmospherically corrected data. However a more significant issue is likely to be the extent to which the extrapolation is required. This assumption for the trend in temperature change past 3.6 km could also result in error in the processed data. A final issue with Researcher is the lack of user accessibility to the atmospheric correction algorithm it employs. Researcher only give an operator the option to define values for ambient temperature and relative humidity. The lack of accessibility means the operator has little to no knowledge of the actual process and components that the atmospheric correction algorithm employs.

It is therefore important to assess the accuracy of data produced using ThermaCam Researcher and to examine other atmospheric correction models which may produce more accurate results.

Methodology

In order to address the results produced by the Researcher atmospheric correction, data collected by the EMCT were analysed using the Ganci et al. (2013) work flow and compared to results produced using the PCModWin MODTRAN interface. In addition, the effect of changes in ambient temperature and relative humidity to transmittance and radiance was also examined using the MODTRAN. A single image (taken at midnight on the 29th) was selected from the August 29 paroxysmal dataset for analysis.

The selected image was processed using the Ganci et al. (2013) workflow to produce a plot of temperature (in Kelvin) over distance for a selected warm pixel using ThermaCam Researcher. Input values used for ambient temperature (21.17 °C) and relative humidity (50.67 %) were collected at an atmospheric station at Primoti, located approximately 1 km away from the EMCT.

Next, MODTRAN was used to calculate atmospheric corrections for the data using the MODTRAN model. Unlike Researcher, MODTRAN allows the operator to customize the atmospheric correction model by providing the options of either entering recorded atmospheric conditions or selecting built-in predefined conditions. A horizontal path-length model and user-defined atmospheric layer were selected and values recorded at the Primoti station for ambient temperature, relative humidity and pressure were used as inputs. Other options, such as CO_2 content, water column density, and band model were left at MODTRAN defaults. The horizontal path length altitude was set at 1.158 km which is the elevation at which the EMCT is positioned. Finally, the spectral wavelength range for the EMCT was defined (7.5 to 13 µm) and a final path length distance of 10 km was selected, with transmittance values calculated at 1 meter and then every 100 meters up to 10,000 meters.

At sensor radiance values for the central wavelength, λ = 10.25 µm, were calculated from the EMCT temperature data using Planck's equation,

$$L_{\lambda} = \frac{2hc^2}{\lambda^5} \frac{1}{(e^{\frac{hc}{\lambda kT}} - 1)}$$

where c is the speed of light in the medium, h is the Planck constant, k is the Boltzmann constant, and T is temperature in Kelvin. Radiance values were then corrected for Ɛ, and atmospheric transmissivity, using the atmospheric transmittance values calculated from MODTRAN,

$$L_{\lambda_{corrected}} = \frac{(\frac{L_{\lambda}}{\tau})}{\varepsilon}$$

where L_{λ} is radiance and τ is transmittance. Finally, the corrected value for radiance was used to calculate temperature using the Planck's equation rearranged to solve for surface temperature,

$$T = \frac{\frac{hc}{k}}{\lambda(ln \frac{\frac{2hc^2}{L_{\lambda}}}{\lambda^5} + 1)}$$

In addition, a second method widely used to calculate surface radiance for TIR data from satellite-based sensors using MODTRAN (French et al., 2003) was also examined,

$$L_{\lambda,srf} = \frac{L_{\lambda,sns} - L_{\lambda,\uparrow}}{\tau} - (1 - \varepsilon)L_{\lambda,\downarrow}$$

where $L_{\lambda,sns}$ is the radiance at the sensor, $L_{\lambda,\uparrow}$ is the upwelling radiance, and $L_{\lambda,\downarrow}$ is the down welling radiance. In order to use this method, however, values for upwelling and down welling radiance are needed. In order to calculate upwelling and down welling radiance, a web-based atmospheric correction parameter calculator was used (Barsi et al., 2003; 2005). The tool required the date and time of acquisition, location (Lat/Long.), a selected upper atmosphere model, surface conditions (altitude, temperature, relative humidity, pressure), and a spectral band curve selection based on either Landsat 5,7, or 8.

Once a temperature curve was calculated from both methods using the recorded atmospheric conditions, additional simulations were carried out to assess the sensitivity to ambient temperature and relative. For ambient temperature, a +/- 30 % range based on the recorded temperature was used. The range was then rounded to the nearest multiple of 5 so that a 5 degree step could be used. This created a range with a minimum of 15 ^{o}C and a maximum of 25 ^{o}C. A similar range was produced for relative humidity, with values rounded to the nearest multiple of 10 to allow a step of 10. This gave a range with a minimum of 40% and a maximum of 70%.

Results

A comparison of results produced using the MOTRAN model with both radiance calculation methods showed good agreement in overall trend (Fig. 2). Temperature values produced using the French et al. (2003) method were slightly lower than those produced using the Planck method. The results produced using MODTRAN and those created using ThermaCam Researcher were compared against one another. While the curves produced using MODTRAN did not fit the regression curve used by Ganci et al. (2013) for the Researcher data, the curves provided a good boundary as relative humidity increased (Fig. 3).

Discussion

Both methods used with MODTRAN produced reasonable results when compared to the regression curve used by Ganci et al. (2013). There are several factors that could account for the discrepancies seen between the MODTRAN curves and the Ganci et al. extrapolated regression curve. One of the primary differences is in the type of atmospheric correction applied to the data. Ganci et al. used ThermaCam Researcher, which uses the LOWTRAN model which is an older atmospheric model. MODTRAN is a newer model and incorporates additional atmospheric parameters than LOWTRAN. However, MODTRAN is mainly used when correcting for satellite-based sensors, while LOWTRAN, even though it is considered obsolete, is still used widely with ground-based cameras.

Unlike MODTRAN, LOWTRAN does not allow any off the correction options to be seen or accessed by the user. Because so much of the correction model can be specified by the operator when using MODTRAN, it is important to have a clear understanding of what each operation does. In the case of this research, the limited duration of the project did not allow enough time for an in depth examination of definable inputs. As a result, several of these options were left as the default MODTRAN option.

Several other issues were found within the processing methods used to calculate temperature with the MODTRAN model. The most significant of these issues occurred when applying the upwelling and down welling radiance in the French et al. (2003) method. In order to do this, the Barsi et al. (2003; 2005) web-based calculator was used. However, because the calculator was designed for use with the Landsat systems, the spectral band range definition followed their image operating parameters. This forced the user to select one of three predefined band models. Since these band models were different from the spectral range on the EMCT, it was likely that resulting temperature calculations would be different than those produced using the EMCT spectral range. Analysing the two methods showed that results produced using upwelling and down welling radiance calculated from the web-based calculator gave lower temperature values than those produced using the Planck method.

As seen in figure 3, the second order polynomial regression curve used by Ganci et al. (2013) does not fit well with the temperature curves produced using MODTRAN. Examining the output curves created using MODTRAN show that both the Planck and French et al. (2003) methods produced very similar trends. These trends were also well matched by exponential regression curves. When an exponential regression curve was used to fit the Ganci et al. data, the curve and the MODTRAN data agreed well when extrapolating temperature values past the Researcher correction limit (Fig. 4).

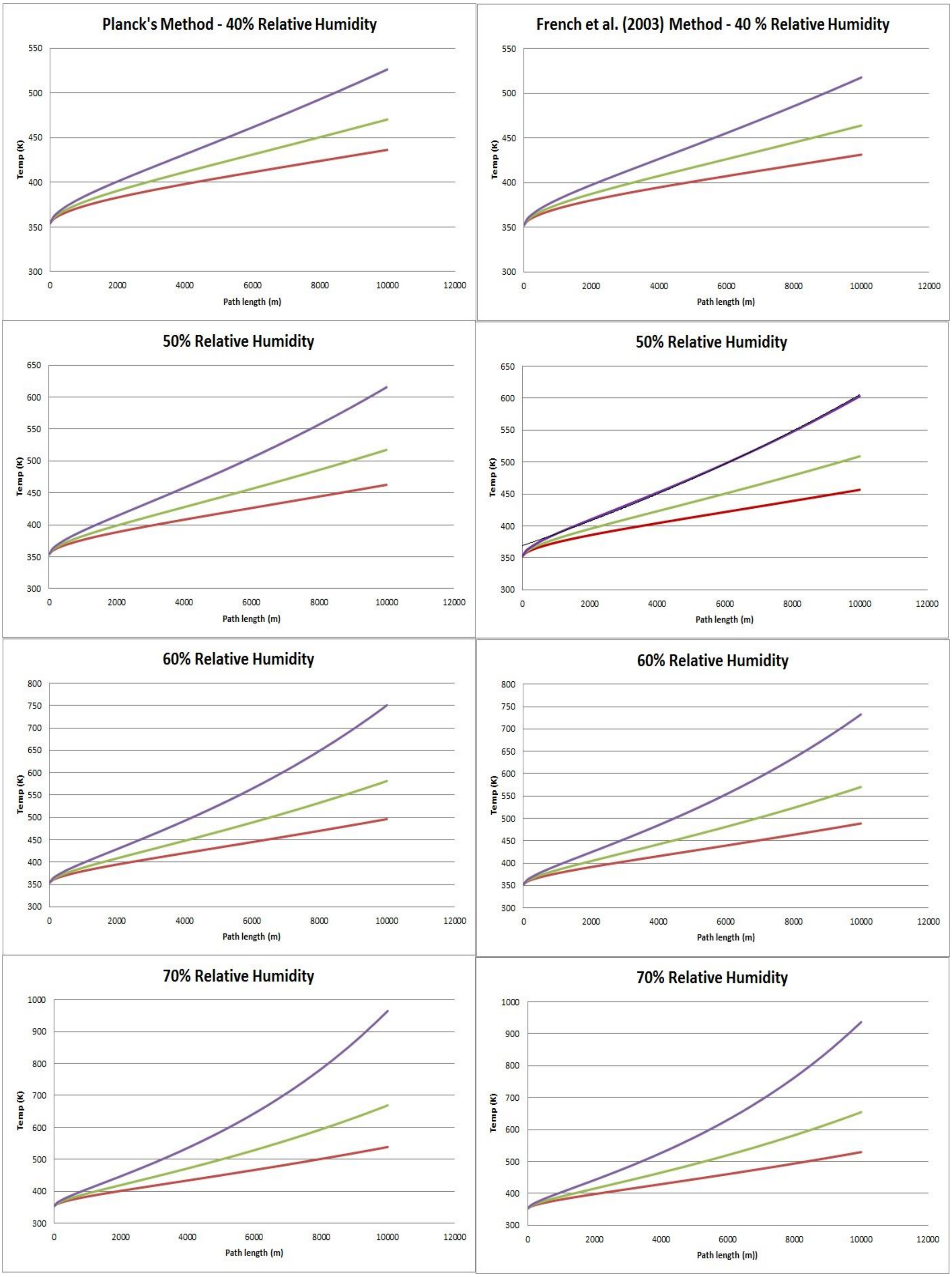

Figure 2 – Comparison of Temperature curves produced using atmospheric transmissivity values taken by MODTRAN: Purple line = 25 °C, Green line = 20 °C, Red line = 15 °C.

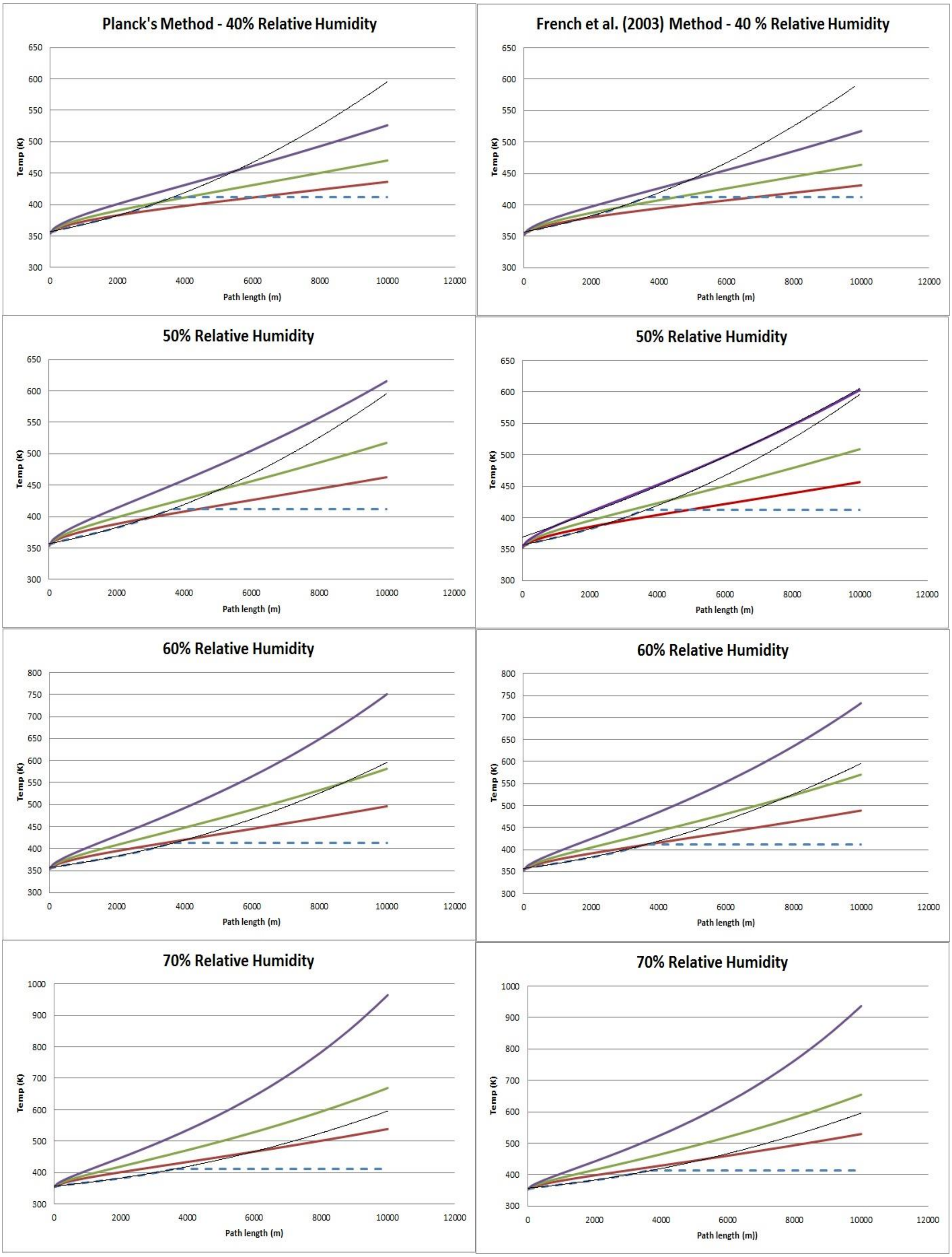

Figure 3 – Comparison of MODTRAN curves with Ganci et al. (2013) regression curve produced using the EMCT temperatures taken at the recorded ambient temperature (21.17 °C) and relative humidity (50.67 %): Dotted blue line = EMCT temperatures, Black line = Ganci et al. (2013) regression curve, Purple line = 25 °C, Green line = 20 °C, Red line = 15 °C.

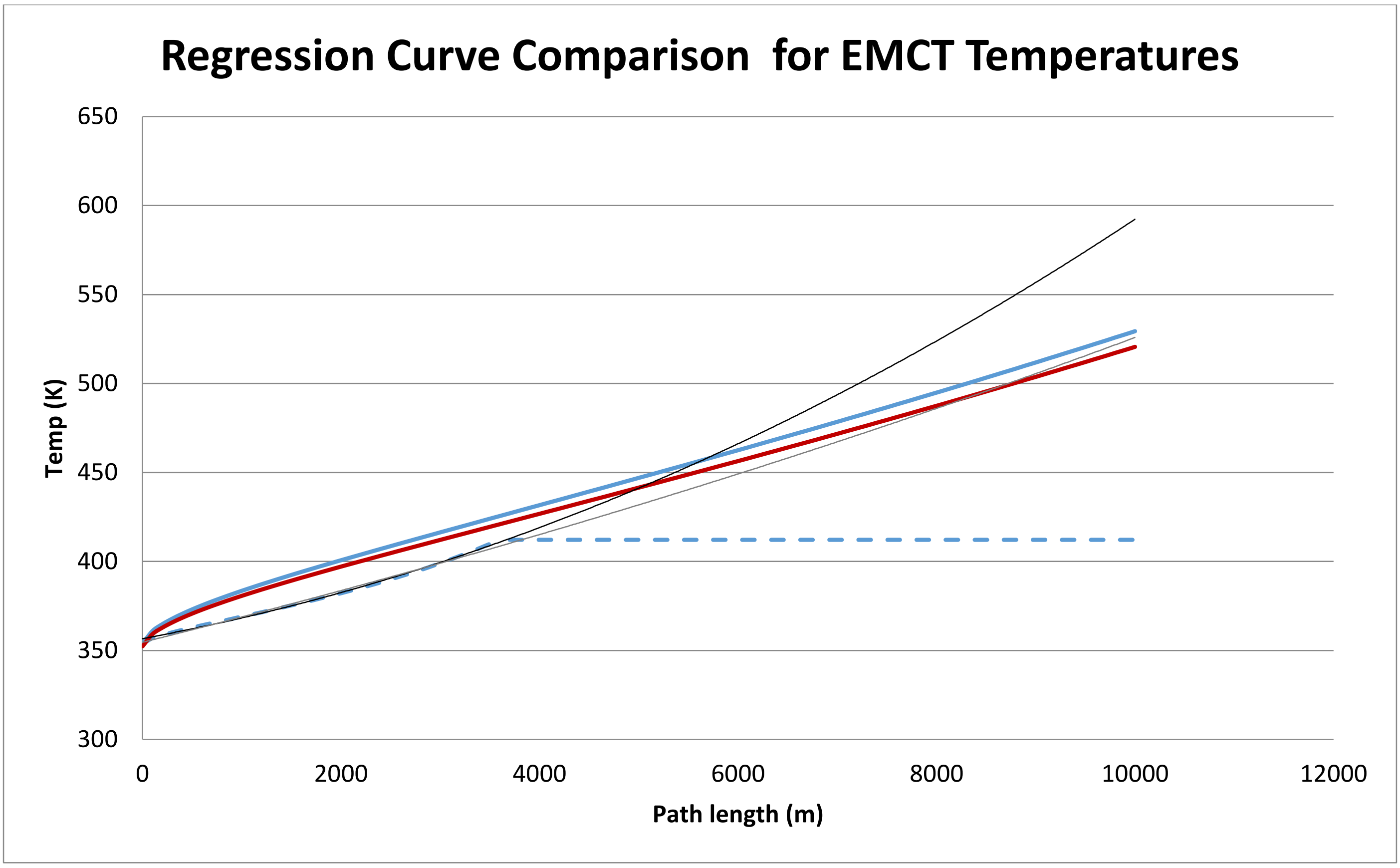

Figure 4 – Comparison of 2nd order polynomial regression curve (Ganci et al., 2013) to exponential regression curve: Blue line = temperature calculated using the Planck's method, Red line = temperature calculated using the French et al. (2003) method, Dotted blue line = EMCT temperatures, Black line = Ganci et al. 2nd order polynomial regression curve, Grey line = exponential regression curve.

Conclusion

Both ThermaCam Researcher and MODTRAN have negative and positive qualities. Both produced reasonable results, and data created using transmittance calculated by MODTRAN with the Planck method and French et al. (2003) method produced similar trends. While the regression curve used by Ganci et al. (2013) did not provide a match to the data created using MODTRAN, the use of an exponential regression curve resulted in a well-matched trend between the Researcher temperature profile and those produced using MODTRAN.

This study provided a good initial examination of these issues. The next step in this research will be to apply the methods used in this study to a target hot and cold pixel in the study image. An in-depth analysis of the MODTRAN input variables and what they represent and how they affect the atmospheric correction will be examined as well. Once these steps have been done, the refined process will be used in assessing effusion rate calculation sensitivity to these issues.

References

BARSI, J.A., Baker, J.L., and Schott, J.R. (2003). An Atmospheric Correction Parameter Calculator for a Single Thermal Band Earth-Sensing Instrument. *Proceedings of IEEE*, **0**, 7803-7929.

BARSI, J.A., Schott, J.R., Palluconi, F.D., and Hook, S.J. (2005). Validation of a web-based atmospheric correction tool for single thermal band instruments. *Proceedings of SPIE*, **5882**, 58820E-58820E-7.

FRENCH, A.N., Norman, J.M., and Anderson, M.C. (2003). A simple and fast atmospheric correction for spaceborne remote sensing of surface temperature. *Remote Sensing of the Environment* , **87**, 326-333.

GANCI, G., James, M.R., Calvari, S., and Del Negro, C. (2013). Separating the thermal fingerprints of lava flows and simultaneous lava fountaining using ground-based thermal camera and SEVIRI measurments. *GEOPHYSICAL RESEARCHER LETTERS*, **40**, 1-6.